Supporting Information

Waste to wealth: a sustainable aquaponic system based on residual nitrogen photoconversion

Vahid Khakyzdeh, *[a,b] Rafael Luque,*[c,d] Mohammad Ali Zolfigol, *[b] Hadi Rezaei Vahidian,[b] Hamid Salehzadeh,[b] Vahid Moradi,[e] Ali Reza Soleymani,[f] Ahmad Reza Moosavi-Zare,[g] Kun Xu [a]

[a]*Institut fur Organische Chemie, Albert-Ludwigs-Universitat Freiburg, Albertstrasse 21, 79104 Freiburg, Germany*

[b]*Faculty of Chemistry, Bu-Ali Sina University, Hamedan, 6517838683, Iran.*

[c]*Departamento de Quimica Organica, Universidad de Córdoba, Edif. Marie Curie, Ctra Nnal IV-A, Km 396, E14014 Córdoba, Spain.*

[d]*Department of Chemical and Biomolecular Engineering (CBME), Hong Kong University of Science and Technology (HKUST), Clear Water Bay, Kowloon, Hong Kong.*

[e]*Department of Chemistry, University of Victoria, PO Box 3065, Victoria, Canada V8W 3V6.*

[f]*Department of Applied Chemistry, Faculty of Science, Malayer University, Malayer 65719, Iran*

[g]*Department of Chemistry, University of Sayyed Jamaleddin Asadabadi, Asadabad, 6541835583, Iran.*

* Corresponding author *E-mail addresses*: v.khakyzadeh@basu.ac.ir and zolfi@basu.ac.ir, rafaluque@ust.hk

TABLE OF CONTENTS

Contents ***Page***

Magnetic Photo Catalytic Reactor (MPC Reactor)

Figure 1 demonstrates a three-dimensional view of the MPC reactor apparatus that was designed to oxidize ammonia to nitrate with the capacity of about 3 L. The reactor was consisted of a UV lamp {250W, wavelength range of 280–400 nm and the maximum emission (350mW/cm^2) at 360 nm (measured by a TOPCON UV-R-1 spectroradimeter), placed vertically in center of the reactor. It is noticeable that the walls of the reactor were mirrors to reflex the light throughout the reactor. Thirty six 2.5×1×0.5 cm^3 neodymium block magnets (**Table 1**) were attached to the walls of the reactor to avoid the dispersion of catalyst {$Fe_3O_4@SiO_2@TiO_2$} throughout the solution and to keep it on their surfaces. An air-pump was applied to provide air to the reactor with a constant flow-rate of 3.5 L.min^{-1}.

Table 1. Properties of neodymium block magnets

Tesla	**$_b$H$_c$**		**$_j$H$_c$**		**(BH)$_{max}$**		mw/Cm^3
	KA/m	KOe	KA/m	KOe	Kj/m^3	MGOe	
≥ 1.18	≥ 780	≥ 10.9	≥ 960	≥ 12	≥ 264	≥ 33	≥ 7.40

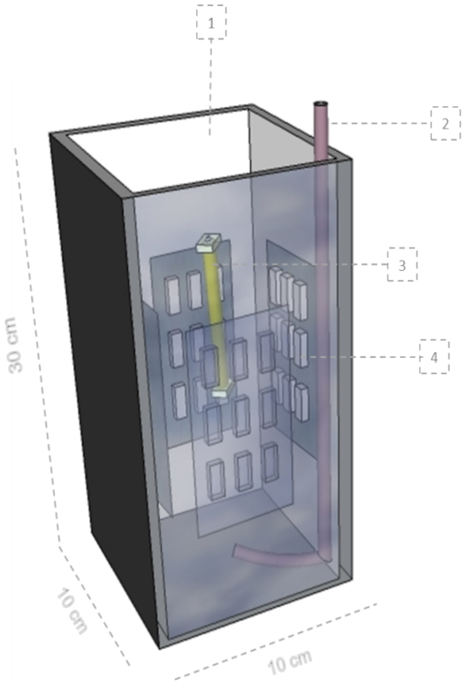

Figure 1. Three-dimensional view of the MPC reactor: 1. Wall of the reactor (mirror); 2. Air pipe attach to an air pomp; 3.UV lamp; 4. Neodymium block magnets.

Micro Aquaponic System (MAS)

As it is shown in **figure 2**, the system was mainly consisted of three parts: (a) fish tank (about 90 L), containing fish (Fish species were tilapia {Oreochromis niloticus}) that were fed three times per day according to the literature [1]. (b) The MPC reactor (**figure 1**) that explained in previous section; (c) the plant tank.

The outlet of fish tank would flow to the reactor by means of the pipe (sign of **A** in **figure 2**). The turbulent current in the pipe could provide the oxygen content by suction of oxygen, which is necessary for the AOP process and the whole system. As it is clear in **figure 2**, the outlet of fish tank is close to the water surface that this situation prevents entering the fish faeces and non-consumed feed to the MPC reactor and plant tank and it would reduce the clogging of the plant roots, which could have adverse effect on crop productivity [2]. In fabrication of the MAS it was found out that the inlet of the MPC reactor should be close to the floor (sign of B in **figure 2**), which leads to more appropriate results. Flowing the water throughout the MPC reactor, ammonia was oxidized to nitrate in front of the catalyst by UV irradiation (the UV-lamp was turned on 1.5 h per day); meanwhile, the AOP method that occur in magnetic photo-catalytic reactor could help to degrade and remove organic pollutants from the water [3]. UV irradiation is a common way to sterilize the aquaponic systems; however its adverse impact is that the irradiation is not selective and damages all bacteria include the beneficial ones (NBs) [4] and this point can be counted as a negative effect on useful bacteria in nitrification step [5]. Since in the present work, no bacteria were utilized for the nitrification step, it did not influence the process. The outlet of the reactor flew to filtering section that was filled with sera^{TM} filter wool and after the filtrations; water was transferred to the plant tank. In this tank, generated nitrate was consumed as a nutrient, which would decrease nitrate concentration. In continues, refined water of the plant tank fell down in next part (section of 11), then the solution was pumped to the fish tank and this cycle was repeated continuously. The flow-rate of water circulated continuously throughout the system was 2 m^3h^{-1}.

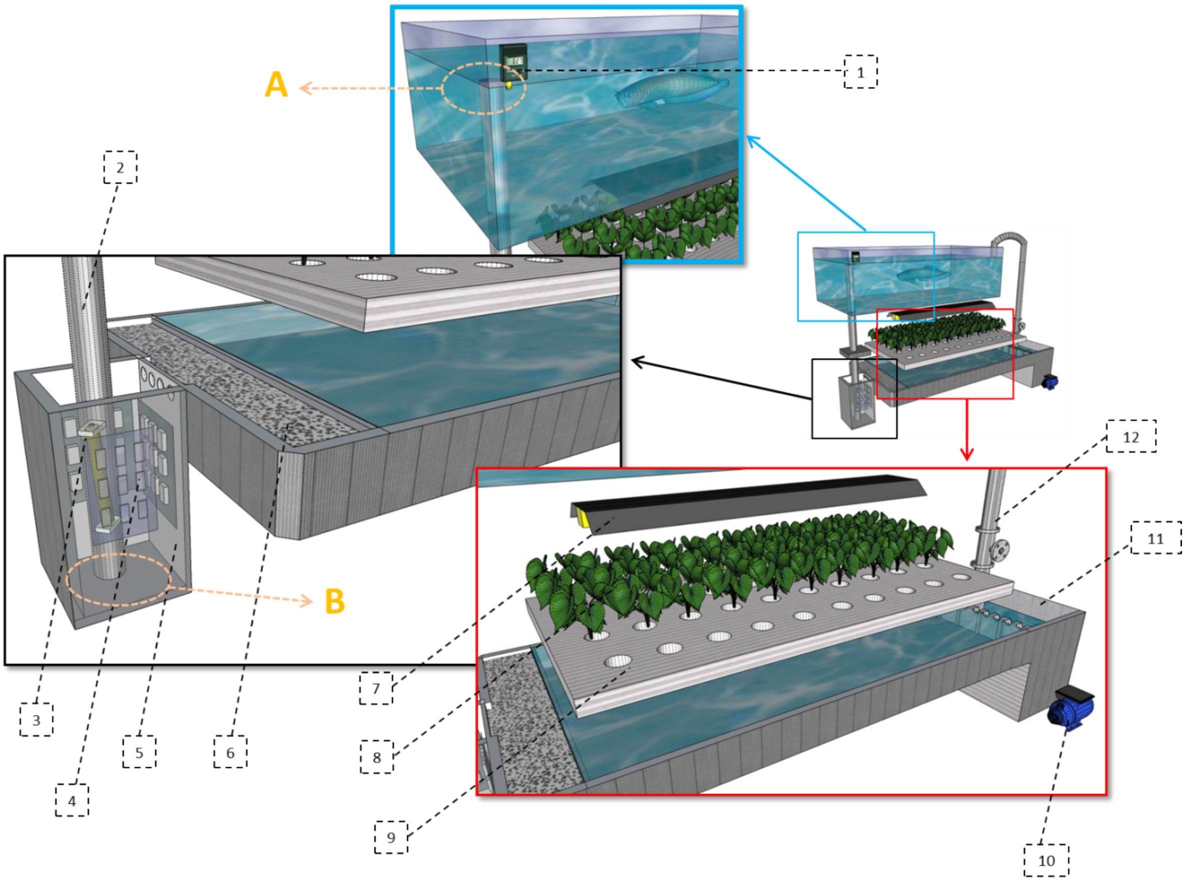

Figure 2. The micro aquaponic system: 1.Thermometer; 2.Pipe; 3. UV lamp; 4. Neodymium block magnet; 5. Mirror; 6. Filtering section; 7. Lamp; 8. Plant; 9. Tank coating of plant breeding; 10. Water pump; 11. Storage reservoir for balance; 12. Tap.

Testing of magnetic photo-catalytic reactor before using of it in the structure of MAS by nitrate concentration measurement

Nitrate concentration measurements were conducted by UV absorption spectrophotometry according to the standard method procedure [6]. Investigations were pursued at 220 nm as the appropriate wavelength. In the case of AOP method and testing the designed reactor, first, 3 g of the catalyst was absorbed uniformly on the surface of magnets (catalyst loading studies were also conducted and 3g was best amount). Then, 2.8 L deionized water containing 8 ppm of the ammonia was added (it should be mentioned that tolerance limit of ammonia for fish (tilapia) is less than 1 ppm [2]). In continues, the UV lamp was switched on to initiate the process at ambient temperature. It should be mentioned that during the AOP method a mild aeration was kept for saturation of water with oxygen. Samples were taken at regular time intervals (15 min) and nitrate generation was investigated using a UV–Vis spectrophotometer.

Obtained results showed that the MPC reactor has the ability to oxidize ammonia to nitrate. As it is presented in **figure 3**, the concentration of nitrate has an intense increasing trend up to 15 min of the process and after that shows a mild increasing trend. The intense increasing trend is due to the high ammonia concentration at the beginning and during the photo-catalytic process it could be oxidized to nitrate rapidly. However, after a while (15 min), the ammonia concentration in the solution decreased, thus, the nitrate concentration increased mildly with respect to the low concentration of the remained ammonia in the solution. Yield of process was 70%.

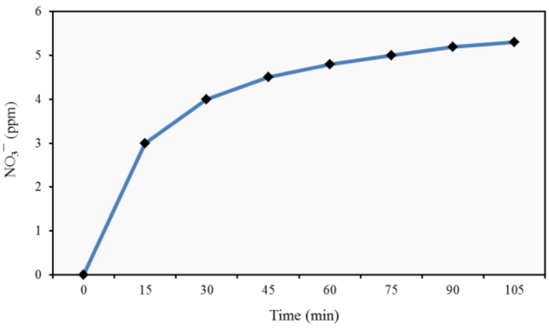

Figure 3. Diagram of the nitrate generation in MPC reactor

Nitrate Concentration Measurement in the MAS

Nitrate concentration measurements were investigated by a selective and reagentless electrode system according to previous report [7]. **Figure 4** shows linear sweep voltammograms for different concentrations of nitrate ion in the range of 0 to 100 ppm on the surface of cupper modified electrode. Peak A_1 is related to reduction of nitrate ion [7]. On the base of showed calibration curve (**figure 4**), nitrate ion concentration was determined in the MAS in period of 30 days.

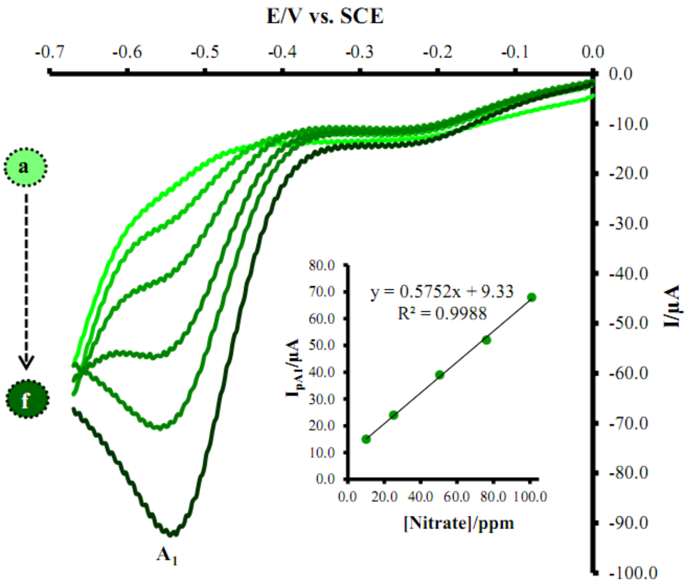

Figure 4. Linear sweep voltammograms for various concentration of nitrate ion on the surface of cupper modified electrode in solution containing 0.1 M Na_2SO_4 (pH = 3.0, HCl). Nitrate concentration from ***a*** to ***f*** are 0, 10, 25, 50, 75 and 100 ppm respectively. Scan rate 100 mVs^{-1}.

Table 2 shows the variation of nitrate concentration within 30 days at intervals of three days. The general range of nitrate concentration in the MAS has been taken between 130– 167 ppm. As it can be observed from **table 2**, the nitrate concentration in the MAS is approximately balanced over time. Interestingly, in several formulations of nutrient solutions (such as; Hoagland solution, Hewitt solution, Cooper solution and Steiner solution) for hydroponic systems, range of amount of nitrate ion was 168 – 210 ppm [8] and amounts of nitrate in designed system was in appropriate level for growth of plants according to standard hydroponic environments.

Table 2. Nitrate concentrations in the MAS

	Day 3	Day 6	Day 9	Day 12	Day 15	Day 18	Day 21	Day 24	Day 27	Day 30
ppm	145	150	140	129	140	140	135	166	156	156

Leaf Area Index

The leaf area growth is depicted in **figure 5**. The Image J 1.46r software was utilized to analyze the images of leaf area. **Figure 5** demonstrates the average growth of the leaf area of the plant in two conditions. As it is observable, the leaf area has increased normally within 32 days in comparison with growth trend in Hoagland solution.

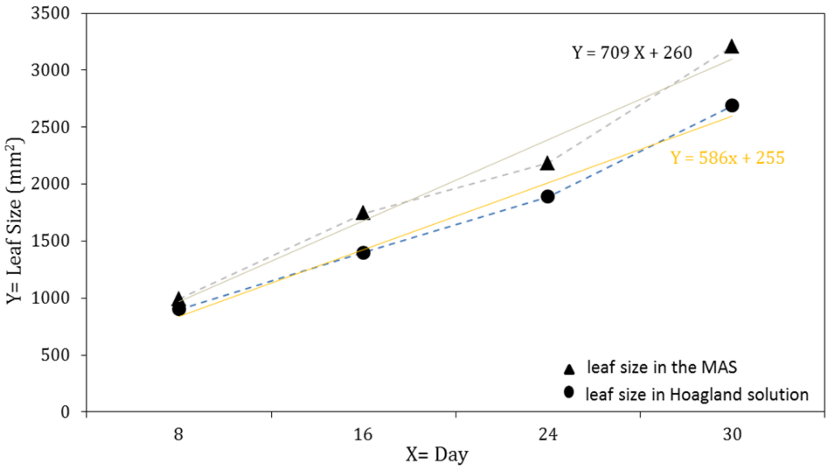

Figure 5. Growth trend of leaf size over time in the MAS.

Surface tension

Figure 6 shows the variation of surface tension with temperature for magnetic and non-magnetic water. As it can be seen, samples containing magnetic water have higher surface tension in different temperatures rather than the non-magnetic water. It is due to the fact that magnetic field stabilize the hydrogen bonds of water molecules. Of course, there is some conflict over the effects of magnetic fields on surface tension. Cho and his co-worker reported that magnetic field reduces the surface tension of natural water about 8% [9] and it has been reported elsewhere that surface tension of water is increased in the presence of a high magnetic field [10]. However, it should be mentioned that surface tension measurements are too sensitive to the media condition, especially to the impurities [11]. The increase in the surface tension at the MAS led to the decrease of the water evaporation, which was advantageous with respect to the water resources.

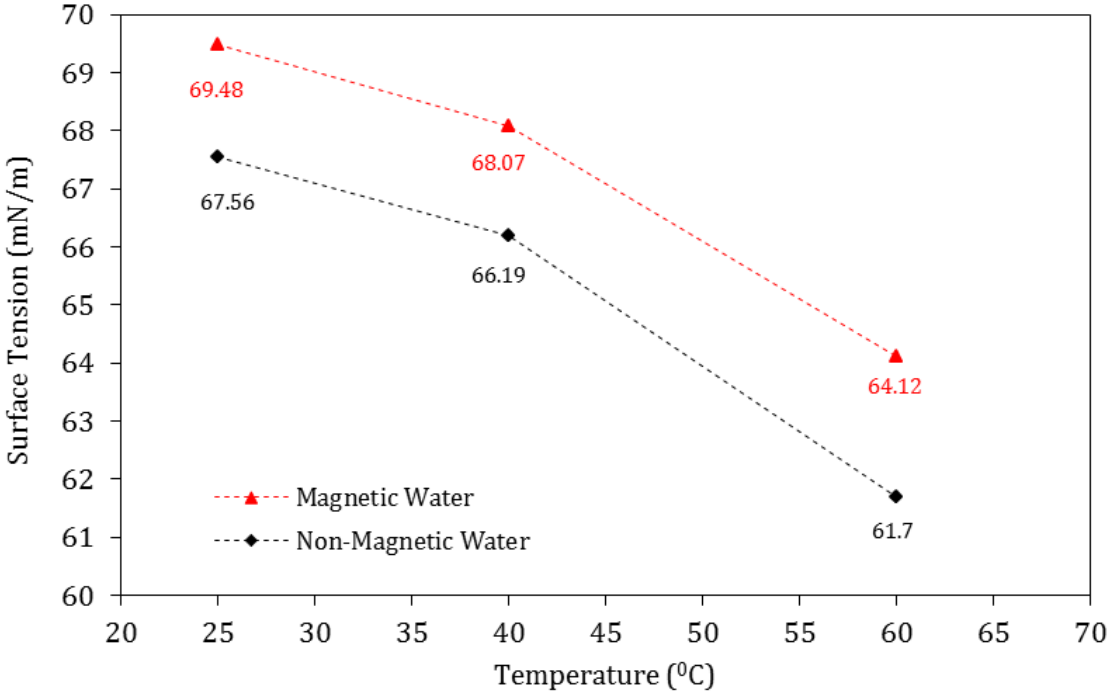

Figure 6. Variation of surface tension versus temperature for magnetic and non-magnetic water at pH ≈ 7.

Viscosity

Figure 7 compares the viscosity of magnetic water and non-magnetic water in different temperatures. It can be observed that the sample with magnetic property is more viscous rather than the sample that was measured 72 h later and has lost its magnetic property. The result is in agreement with the previous reports [12].

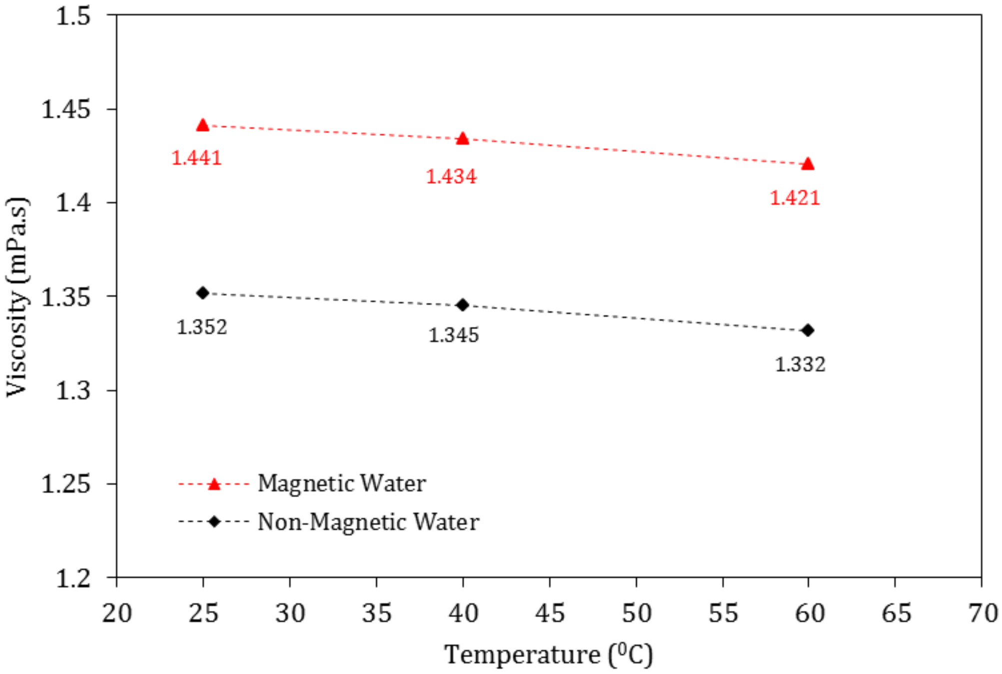

Figure 7. Variation of viscosity versus temperature for magnetic and non-magnetic waterat pH ≈ 7.

Conductivity measurement

The conductivity of a solution depends on the total concentration of the dissolved ions [13]. **Figure 8a, b and c** shows the variation of conductivity before and after the photo-catalytic process within 30 days. As it is observable, the conductivity was always increased when the UV lamp was switched on and the oxidation process was conducted. It can be explained by the fact that when the UV lamp was switched on, oxidation process that resulted to ion generation was started and the higher conductivity achieved. Reduction of conductivity in the next day is related to consumption of ions by plants.

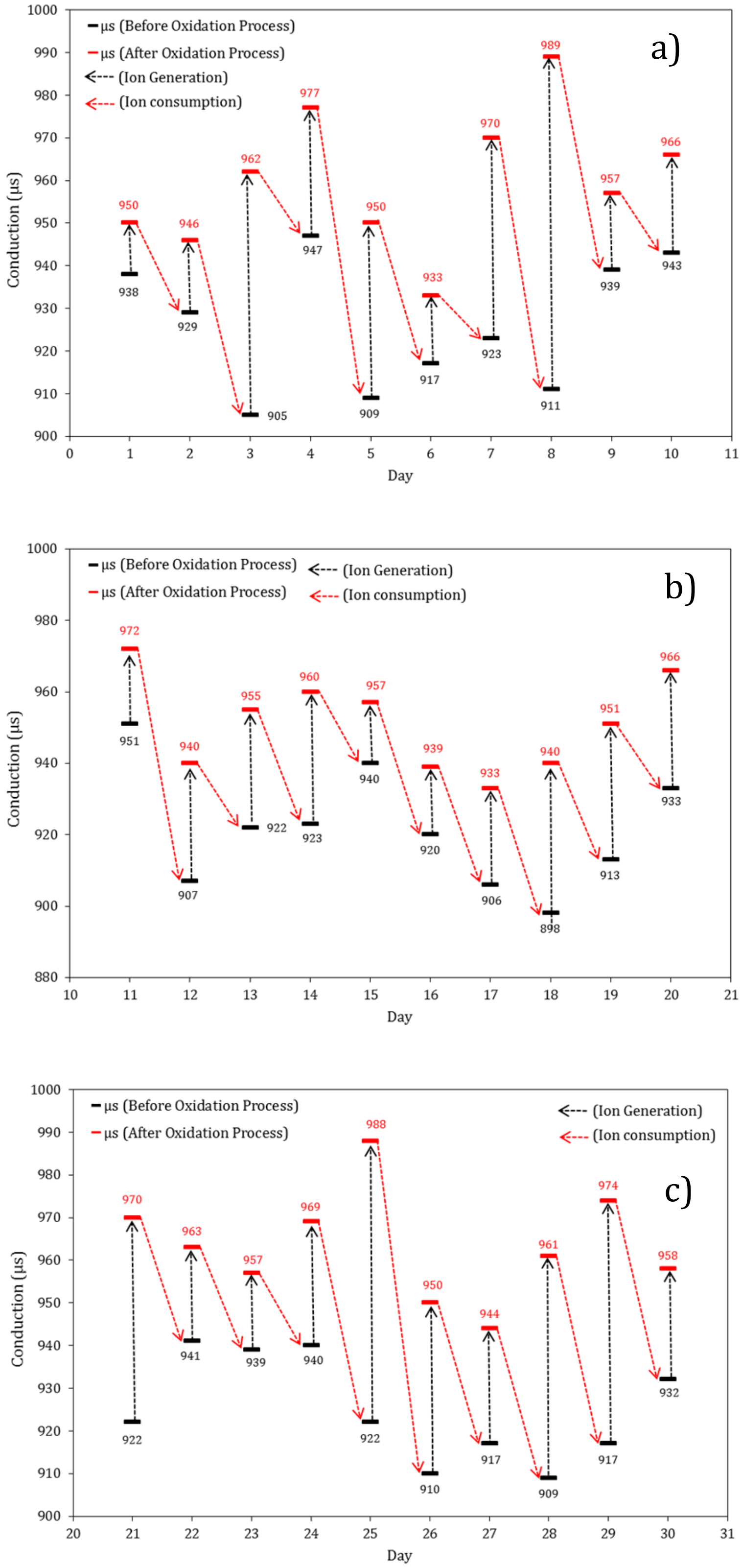

Figure 8. Variation of conductivity before and after the photo-catalytic process at pH ≈ 7 and ambient temperature.

Dissolved oxygen

The dissolved oxygen content was measured for the magnetic water and non-magnetic water using Winkler method according to standard method procedure [6]. The aeration was done within 30 min before the measurement for the complete saturation. As it could be predicted, the dissolved oxygen concentration for the magnetic water (9 ppm) was more than the non-magnetic water (7 ppm).

pH measurement

Since ammonia is basic, an increase in the ammonia concentration would result to an increase in the pH value; thus, the pH value can be measured as a criterion to pursue. As it can be observed from **figure 9**, the pH value is approximately constant (pH ≈ 7). It can be attributed to the fact that the ammonia concentration, produced by wastes, was remained constant during the process; because, ammonia was oxidized to nitrate by the AOP process.

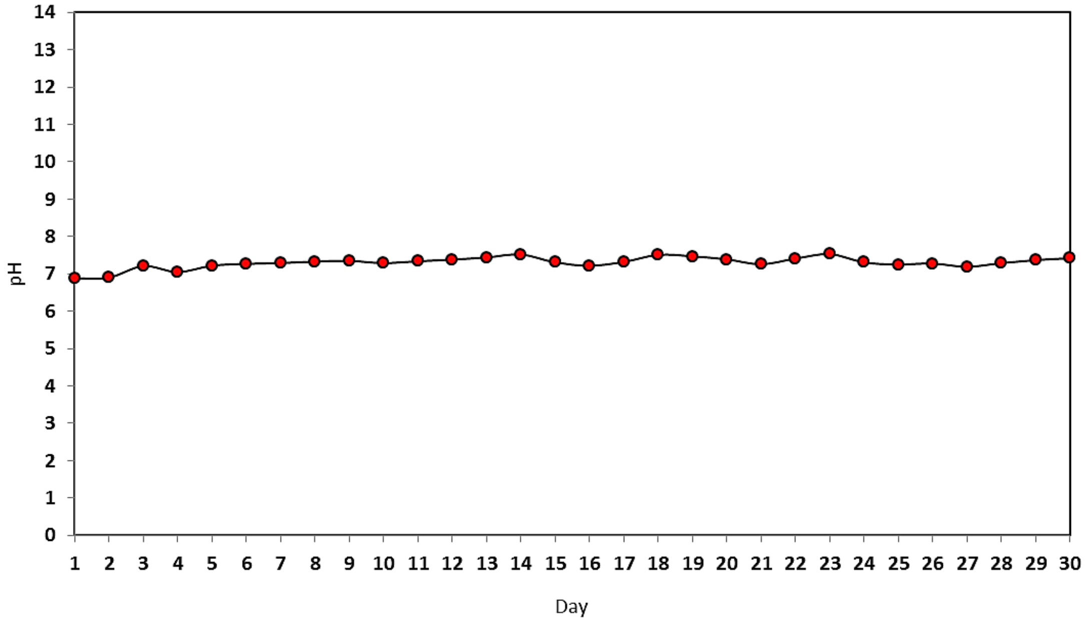

Figur e 9. Variation of pHvalue in the MAS.

Materials and Some general methods

The nitrate concentration was measured by a spectrophotometer (Perkin-Elmer Lambda 45) within 220 nm. The pH was measured by a pH-meter (UB-10 Denver Instruments). The conductivity and the viscosity were measured by a Jenway 4510 Conductivity conductometer and an Ubblelohde viscometer, respectively. The density of samples was measured by means of an Anton Paar DMA 4500 oscillating U-tube densiometer (the uncertainty for density measurements was ±0.01 kg m^{-3}) provided with automatic viscosity correction. Leaf area analysis was conducted with software of Java-based image processing of Image J1.46r developed at the National Institutes of Health.

Surface tension. The drop-volume method according toreported investigations [14] was used to determine the surface tension of the samples. A glass capillary with outer diameter of 4.5 mm, small thickness, which has thinly ground tip to give an angle of 90° between the ground face and the internal bore at the end with the edges sharp, was used. The aqueous phase was kept in a narrow glass syringe that was coupled by an adjustable syringe pump (Phoenix M-CP, French) and flowed through a rigid tube to the capillary in the air. A low flow-rate (1.0 mL in 29 min) of the aqueous phase was conducted to the capillary, and drops were formed slowly at the tip of the capillary. Drop volume measurements were repeated at least six times. The surface tension measurements were carried out at 25.0, 40.0 and 60.0 °C with an uncertainty of 0.1 °C, using an adjustable safe and calibrated thermostat (OPTIMA 740, Japan).Samples of the aqueous phases were separated for the density measurement. The apparatus was calibrated once a day with dry air and deionized water. The desired temperature was self-adjusted in this density-meter with an uncertainty of 0.01 °C. The relationship of samples'surface tension with the volume of drop (v), falling off the capillary, is given by Harkins and Brown [15]. The uncertainty in measurement results is estimated to be within ±0.1 mN m $^{-1}$.

Viscosity. Viscosities were measured with an Ubbelohde viscometer at 25 ^{o}C, 40 ^{o}C and 60 ^{o}C, respectively using Poiseuille'slaw Ubbelohde viscometer according to reported literature [16]. The experiments were repeatable to within $\pm 2\times 10^{-3}$mPa s. The apparatus was calibrated once in a day with dry air and double distilled freshly degassed water.

Catalyst preparation {Fe_3O_4@SiO_2@TiO_2}. Fe_3O_4 particles and Fe_3O_4@SiO_2 were prepared according to our previous reports [17] and the embedding of titania layer into the Fe_3O_4@SiO_2 was conducted according to Jeon procedure [18]. Transmission electron microcopy (TEM) images of Fe_3O_4@SiO_2@TiO_2 nanoparticles are shown in figure 10. Energy dispersive x-ray (EDX) analysis of Fe_3O_4@SiO_2@TiO_2 nanoparticles showed expected elements such as; iron, oxygen, silicon and titanium; spectrum indicated in figure 11. The XRD pattern of Fe_3O_4@SiO_2@TiO_2 nanoparticles were studied and exhibited peaks at 2θ= 25.3, 37.7, 47.9, 53.8 and 62.5 corresponding to diffraction lines (101), (004), (200), (105) and (204), respectively.

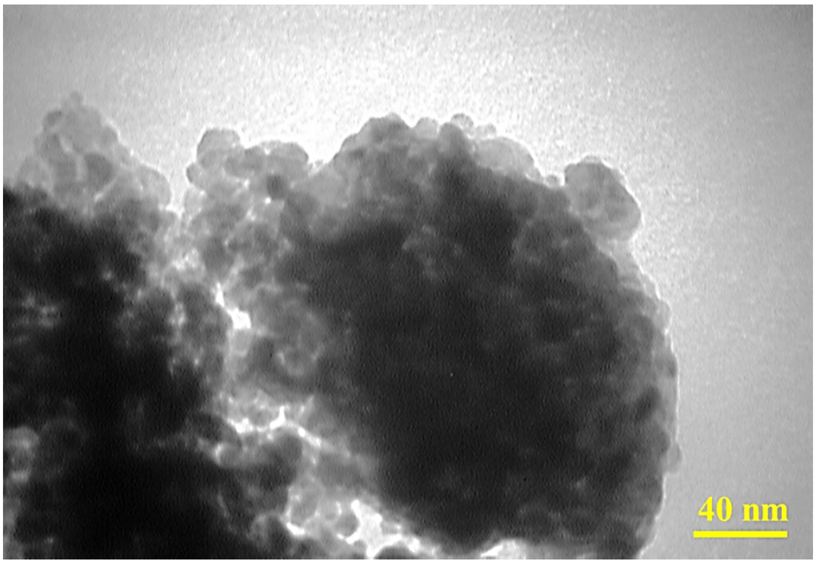

Figure 10. TEM images of Fe_3O_4@SiO_2@TiO_2 nanoparticles

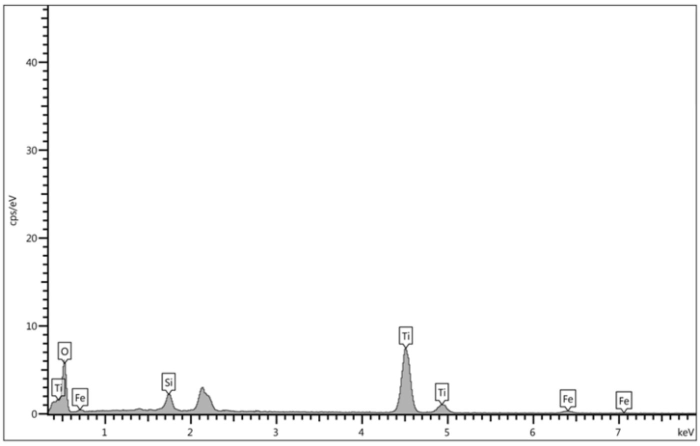

Figure 10. Energy-dispersive X-ray spectroscopy (EDX) of $Fe_3O_4@SiO_2@TiO_2$ nanoparticles

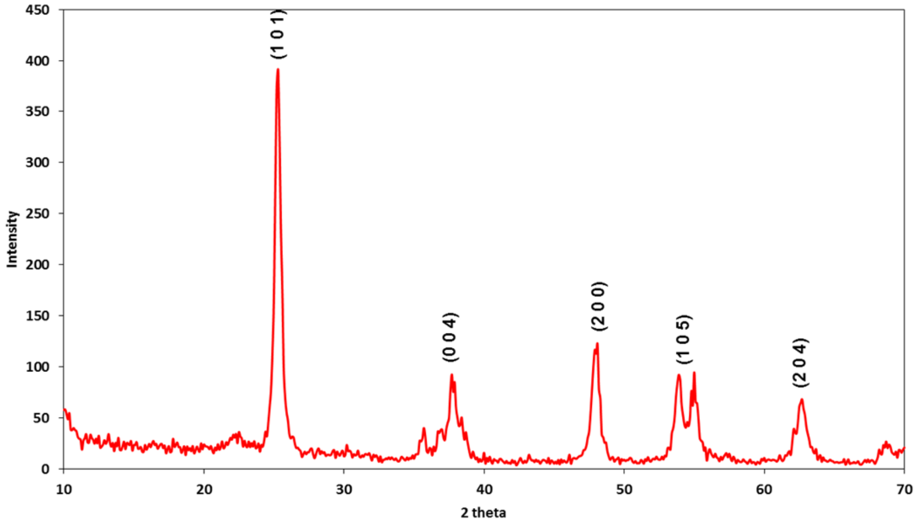

Figure 11. XRD pattern of $Fe_3O_4@SiO_2@TiO_2$ nanoparticles

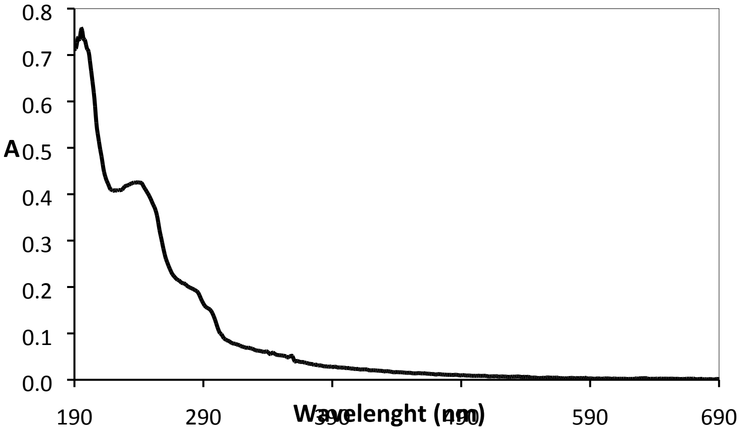

Uv-vis spectrum of $Fe_3O_4@SiO_2@TiO_2$ nano catalyst

References

1- Riche, M. A. & Garling, D. Feeding Tilapia in Intensive Recirculating Systems, USDA North Central Regional Aquaculture Center Fact Sheet, (2003).

2- Graber, A. & Junge, R. Aquaponic Systems: Nutrient recycling from fish wastewater by vegetable production, *Desalination*, **246**, 147-156 (2009).

3- (a) Autin, O., Hart, J., Jarvis, P., Mac Adam, J., Parsons, S. A. & Jefferson, B. Comparison of UV/TiO_2 and UV/H_2O_2 processes in an annular photoreactor for removal of micropollutants: Influence of water parameters on metaldehyde removal, quantum yields and energy consumption, *Appl. Catal., B*, **138**, 268-275 (2013); (b) Zhang, Q., Li, C. & Li, T. Rapid photo-catalyticdecolorization of methylene blue using high photon flux UV/TiO_2/H_2O_2 process, *Chem. Eng. J.* **217**, 407-413 (2013); (c) Simonsen, M. E., Jensen, C. V. & Soogaard, E. G. Comparison of different UV-activated AOP methods, *J. Adv. Oxid. Technol,* **16**, 179-187 (2013); (d) Moreira, F. C., Vilar, V. J. P., Ferreira, A. C. C., dos Santos, F. R. A., Dezotti, M., Sousa, M. A., Gonçalves, C., Boaventura, R. A. R. & Alpendurada, M.F. Treatment of a pesticide-containing wastewater using combined biological and solar-driven AOPs at pilot scale, *Chem. Eng. J.* **209**, 429-441 (2012); (e) Lopes, F. V. S., Monteiro, R. A. R., Silva, A. M. T., Silva, G. V., Faria, J. L., Mendes, A. M., Vilar, V. J. P. & Boaventura, R. A. R. Insights into UV-TiO_2 photo-catalytic degradation of PCE for air decontamination systems, *Chem. Eng. J.* **204**, 244-257 (2012); (f) Yang, J. K., Lee, S. M., Farrokhi, M., Giahi, O. & ShirzadSiboni, M. Photo-catalytic removal of Cr(VI) with illuminated TiO_2, *Desalin. Water Treat*, **46**, 375-380 (2012); (g) Chuang, L. C., Luo, C. H., Chuang, M. C. & Wang, M. C. Degradation of Butylparaben by Ozonation and UV/TiO_2 Processes, *Adv. Mat. Res*, **488**, 159-163 (2012).

4- Mora, D., De Mora, S., Demers, S. & Vernet, M. *The effects of UV radiation in the marine environment* (Cambridge University Press, 2000).

5- (a) Hooper, A. B. & Terry, K. R. Photoinactivation of ammonia oxidation in Nitrosomonas, *J. Bacteriol*., **119,** 899-906 (1974); (b) horrigan, S. G. Carlucci, A. F. & Williams, P.M. Light inhabitation of nitrification in see-surface films, *J. Mar. Res*, **39**, 557-565 (1981).

6- APHA, Standard Methods for the Experimentation of Water and Wastewater, 21st ed., American Public Health Association/American Water Works Association/Water Environment Federation, Washington DC, USA, (2005).

7- Davis, J., Moorcroft, M. J., Wilkins, S. J, Compton, R. G. & Cardosi, M. F. Electrochemical detection of nitrate and nitrite at a copper modified electrode, *Analyst*, **125**, 737–742 (2000).

8- Trejo-Téllez, L I. & Gómez-Merino F. C, Nutrient Solutions for Hydroponic Systems, Hydroponics - A Standard Methodology for Plant Biological Researches, (2012).

9- Cho Y. I. & Lee, S.-H. Reduction in the surface tension of water due to physical water treatment for fouling control in heat exchangers, *Int. Commun. Heat Mass Transfer*, **32**, 1-9 (2005).

10- (a) Fujimura, Y. & Iino, M. The surface tension of water under high magnetic fields, *J. Appl. Phys*. **103**, 124903-124904 (2008); (b) Toledo, E. J. L., Ramalho, T. C. & Magriotis, Z.M. Influence of magnetic field on physical–chemical properties of the liquid water: Insights from experimental and theoretical models. *J. Mol. Struct.* **888**, 409-415 (2008); (c) Fujimura Y. & Masaaki, I. The surface tension of water under high magnetic fields. *J. App. Phys.* **103**, 124903-124906 (2008); (d) Masaaki I. & Fujimura, Y. Surface tension of heavy water under high magnetic fields, *Appl. Phys. Lett.* **94**, 261902-261904 (2009).

11- Amiri M.C. & Dadkhah, A. A. On reduction in the surface tension of water due to magnetic treatment, *Colloids Surf*., **278**, 252-255 (2006).

12- (a) Ghauri, S. & Ansari, M. Increase of water viscosity under the influence of magnetic field. *J. Appl. Phys*. **100**, 066101-066102 (2006); (b) Iwasaka, M. & Ueno, S. Structure of water molecules under 14 T magnetic field. *J. Appl. Phys*. **83**, 6459-6461 (1998); (c) Hosoda, H., Mori, H., Sogoshi, N., Nagasawa, A. & Nakabayashi, S. Refractive Indices of Water and Aqueous Electrolyte Solutions under High Magnetic Fields. *J. Phys. Chem*. **108**, 1461-1464 (2004); (d) Inaba, H., Saitou, T., Tozaki, K. & Hayashi, H. Effect of the magnetic field on the melting transition of H_2O and D_2O measured by a high resolution and supersensitive differential scanning calorimeter. *J. Appl. Phys.* **96**, 6127-6132 (2004).

13- Lepetit, J., Sale, P., Favier, R. & Dalle, R. Electrical impedance and tenderisation in bovine meat, *Meat Science,* **60**, 51–62 (2002).

14- (a) Saien, J. & Asadabadi S. Adsorption and Interfacial Properties of Individual and Mixtures of Cationic/Nonionic Surfactants in Toluene Water Chemical Systems. *J. Chem. Eng. Data*. 55, 3817–3824 (2010); (b) Saien, J., Riazikhah, M. & Ashrafizadeh, S. N. Comparative investigations on the effect of contaminants and mass transfer direction in liquid-liquid extraction. *Ind. Eng. Chem. Res*. 45, 1434–1440 (2006).

15- Saien, J. & Asadabadi S. Synergistic adsorption of Triton X-100 and CTAB surfactants at thetoluene + water interface. *Fluid Phase Equilib*. **307**, 16– 23 (2011).

16- Iloukhani, H. Rezaei-Sameti, M & Zarei H.A. Volumetric and viscometric studies of molecular interaction of the ternary system toluene (1) + cyclohexane (2) +n-hexane (3) at 298.15 K. *Thermochim. Acta*, **438**, 9–15 (2005).

17- (a) Zolfigol, M. A., Khakyzadeh, V., Moosavi-Zare, A. R., Rostami, A., Zare, A., Iranpoor, N., Beyzavi, M. H. & Luque, R. A highly stable and active magnetically separable Pdnanocatalyst in aqueous phase heterogeneously catalyzed couplings. *Green Chem*, **15**, 2132-2140 (2013); (b) Koukabi, N., Kolvari, E., Khazaei, A., Zolfigol, M. A., Shirmardi-Shaghasemi, B. & Khavasi, H. R. Hantzsch reaction on free nano-Fe_2O_3 catalyst: excellent reactivity combined with facile catalyst recovery and recyclability. *Chem. Commun*, **47**, 9230–9232 (2011).

18- Joo, J., Ye, Y., Kim, D., Lee, J. & Jeon S. Magnetically recoverable hybrid TiO_2 nanocrystal clusters with enhanced photo-catalytic activity. *Mater. Lett.* **93**, 141–144 (2013).